In vivo and *in vitro* induction of the apoptotic effects of oxysophoridine on colorectal cancer cells via the Bcl-2/Bax/caspase-3 signaling pathway

SHAO-JU JIN[1*], YUN YANG[2*], LEI MA[3*], BEN-HUI MA[1], LI-PING REN[1], LIU-CHENG GUO[1], WEN-BAO WANG[1], YAN-XIN ZHANG[1], ZHI-JUN ZHAO[1] and MINGCHEN CUI[1,4]

[1]Department of Pharmacology, The First Affiliated Hospital, Luohe Medical College, Luohe, Henan 462002; [2]Department of General Surgery, The First Affiliated Hospital of Nanchang University, Nanchang, Jiangxi 330006; [3]Department of Emergency, General Hospital of Ningxia Medical University, Yinchuan, Ningxia 750004; [4]Tumor Occurrence and Prevention Research Innovation Team of Luohe, Luohe Medical College, Luohe, Henan 462002, P.R. China

Abstract. Oxysophoridine (OSR) is a major active alkaloid extracted from *Sophoraalopecuroides* L. The aim of the present study was to investigate the induction of the apoptotic effects of OSR on colorectal cancer cells *in vivo* and *in vitro*. The results of the MTT and colony formation assays demonstrated that the proliferation of HCT116 cells was inhibited by OSR *in vitro*. The characteristics of cellular apoptosis in OSR-treated HCT116 cells were analyzed by Hoechst 33258 staining. It was also observed that the expression of caspase-3, B-cell lymphoma-2 (Bcl-2) associated X protein (Bax) and cytochrome *c* increased significantly upon OSR treatment. However, the expression of Bcl-2 and poly ADP-ribose polymerase-1 (PARP-1) was downregulated in OSR-treated cells compared with untreated cells. The *in vivo* experiments identified that OSR significantly inhibited the growth of the transplanted mouse CT26 tumor tissue, upregulated the expression of caspase-3, Bax and cytochrome *c* and downregulated the expression of Bcl-2 and PARP-1, as detected by reverse transcription-quantitative polymerase chain reaction and western blotting. It may be concluded that OSR significantly induced apoptotic effects on colorectal cancer cells *in vivo* and *in vitro*, and that its mechanism may be associated with the Bcl-2/Bax/caspase-3 signaling pathway.

Introduction

Colorectal cancer (CRC) is one of the most common gastrointestinal malignancies worldwide (1,2). In previous years, with the improvement of living conditions, increases in lifespan and alterations to environmental pollution factors, the morbidity and mortality of colorectal cancer has increased significantly, alongside a decrease in the age of disease onset (3-5). The pathogenesis of colorectal cancer is complex, and therefore diagnosis is often difficult in the earlier stages of disease (6). At present, surgery, chemotherapy and radiotherapy are the most effective treatments, and the primary methods used to treat colorectal cancer (7). However, the success rate of this therapy is not sufficient, and the rate of CRC mortality is increasing year by year (8,9), which indicates that innovative strategies are required to control this deadly disease.

A number of previous studies have reported the potential anti-tumor activities of various herbal medicines in various experimental models of cancer (10-12). Clinical reports have also demonstrated the beneficial effects of herbal medicines in patients with tumors (13,14). Therefore, it is necessary to identify novel drugs for the prevention and treatment of tumors.

Oxysophoridine (OSR) is a major active alkaloid extracted from *Sophoraalopecuroides* L. (15). The chemical structure of OSR comprises two piperidine rings (Fig. 1), and it belongs to the family of quinolizidine alkaloids. OSR has been identified to possess several pharmacological activities such as anti-oxidative and anti-inflammatory effects, suppression of the growth of hepatocellular carcinoma and analgesic and central inhibitory effects (16-20). However, the anti-tumor potential of OSR in CRC has not been characterized. Therefore, the present study aimed to investigate the anti-tumor effects of OSR in CRC and to investigate the induction of the apoptotic effects of OSR in the CRC HCT116 cell line and mouse CT26 tumor model. The findings of the present study suggest that

Correspondence to: Professor Mingchen Cui, Department of Pharmacology, The First Affiliated Hospital, Luohe Medical College, 148 Daxue Road, Luohe, Henan 462002, P.R. China
E-mail: 14890698@qq.com

Dr Yun Yang, Department of General Surgery, The First Affiliated Hospital of Nanchang University, 17 Yongwaizheng Street, Nanchang, Jiangxi 330006, P.R. China
E-mail: march11yang@163.com

*Contributed equally

OSR mediates its anti-colorectal cancer activity via the regulation of the B-cell lymphoma 2 (Bcl-2)/Bcl-2-associated X protein (Bax)/caspase-3 signaling pathway to induce apoptosis *in vitro* and *in vivo*.

Materials and methods

Cell culture and experimental reagents. Colorectal cancer HCT116 and CT26 cell lines were purchased from Nanjing Keygen Biotech Co., Ltd. (Nanjing, China). Cells were maintained in Dulbecco's modified Eagle's medium (DMEM)/high glucose medium (Invitrogen; Thermo Fisher Scientific, Inc., Waltham, MA, USA) supplemented with 12% heat-inactivated fetal bovine serum (Minhai Biological Engineering Co., Ltd., Lanzhou, China), and 1% penicillin-streptomycin (Sigma-Aldrich; Merck KGaA, Darmstadt, Germany), and cultured at 37°C in a humidified atmosphere of 5% CO_2. When the concentration of cells reached $1x10^5$ cells/ml for subculture the treatments were performed and all experiments were performed with cells in the logarithmic phase of growth. OSR was extracted from *Sophoraalopecuroides* L. (purity ≥98%; Chengdu Herbpurify Co., Ltd., Chengdu, China) and dissolved in normal saline (NS) at an initial concentration of 200 mg/ml and stored at -20°C. Fluorouracil (5-Fu) was obtained from Shanghai Xudong Haipu Pharmaceutical Co., Ltd., Shanghai, China. Primary antibodies against caspase-3, cytochrome *c*, Bcl-2, Bax and poly (adenosine 5'-diphosphate-ribose) polymerase 1 (PARP-1) were purchased from Santa Cruz Biotechnology, Inc. (Dallas, TX, USA). Trypsin and MTT were obtained from Sigma-Aldrich; Merck KGaA.

Assessment of cell growth inhibition ratio. To assess cell growth inhibition ratio, HCT116 cells ($5x10^3$) were seeded into 96-well plates (Guangzhou Jet Bio-Filtration, Co., Ltd., Guangzhou, China). Following overnight incubation at 37°C, different concentrations of OSR (3, 6, 12, 24, 48, 96 and 192 mg/l) were used to treat the cells, and the cells were incubated at 37°C for 48 h (6 wells for each concentration). Briefly, 20 μl MTT solutions (5 mg/ml) was added to each well and incubated for 4 h at 37°C, then 150 μl dimethyl sulfoxide was added to each well to dissolve MTT formazan, and the plate was shaken at room temperature for 15 min. The absorbance was measured at 490 nm with a microplate reader (Bio-Rad Laboratories, Hercules, CA, USA). The half maximal inhibitory concentration (IC_{50}) was calculated using SPSS version 17.0 (SPSS, Inc., Chicago, IL, USA).

Growth curve assay. To evaluate the cell growth curve, HCT116 cells ($1x10^3$ cells/well) were inoculated into 96-well plates. After 24 h, the cells were treated with OSR at different concentrations (100, 50, and 25 mg/l) for 1 to 7 days. The control group was incubated in a drug-free medium, and the positive group was exposed to 5-Fu (20 mg/l) (21). The number of surviving cells from each group was counted daily using Trypan Blue staining assay, according to the directions below. A total of 10 μl 0.4% Trypan Blue solution was added to 90 μl of cell-suspension with sufficient mixing, and 10 μl solution was added on to the cell-count boards. Cells were then counted to assess the number of viable cells, under a light microscope (Olympus CX31) at x10 magnification.
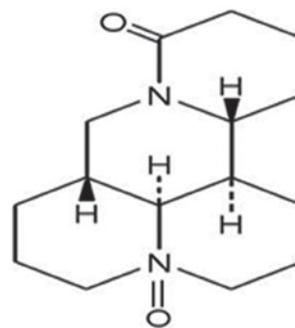
Figure 1. Molecular structure of oxysophoridine.

Colony formation assay. For the colony formation assay, 200 cells were seeded into 6-well plates and exposed to various concentrations of OSR (100, 50 and 25 mg/l) for 14 days at 37°C in 5% CO_2 atmosphere with a relative humidity of 95%. The colonies were fixed in pure methanol solution at room temperature for 15 min and then stained with Giemsa (3%) at room temperature for 30 min and washed 3 times with PBS, 5 min/time. Images of the colonies were captured and counted under a light microscope, and the colony formation inhibitory rate was calculated as follows: (1-mean number of colonies in the OSR group/mean number of colonies in the negative control group) x100.

Hoechst 33258 staining assay. The HCT116 cells were seeded at a density of $5x10^3$ cells/ml into a 24-well plate. After 24 h, the cells were treated with OSR at various concentrations (100, 50, and 25 mg/l) for 48 h. The cells were washed with PBS three times, fixed with 4% neutral paraformaldehyde at room temperature for 30 min, washed with PBS three times and stained with 2 mg/l Hoechst for 30 min at room temperature. The chromatin structure of the cells was observed by fluorescence microscopy at x200 magnification, and the apoptosis rate was calculated as follows: Apoptosis rate (%) = apoptosis cell number/(normal cell number + apoptosis cell number) x100.

RNA isolation and reverse transcription-quantitative polymerase chain reaction (RT-qPCR). Total RNA was isolated from treated cells or tissues with TRIzol® reagent (Bio Basic, Inc., Markham, ON, Canada), according to the manufacturer's protocol. Total RNA was reverse transcribed with the RevertAid™ First Strand cDNA Synthesis kit (Fermentas; Thermo Fisher Scientific, Inc.) according to manufacturer's protocol. A total of 2 μl RNA samples were diluted by DEPC water, and the absorbance value (A) of RNA solution was detected by UV spectrophotometer at 260 and 280 nm respectively. The purity of RNA samples was determined according to the ratio of A260 nm/A280 nm. A ratio between 1.8-2.0, indicates that the purity of the RNA samples are high, whereas <1.8 demonstrates that the samples are contaminated by protein, and >2.0 demonstrated that the samples have RNA degradation. Primer sequences of all the genes are listed in Table I. A total reaction volume of 25 μl was used, composed of 2 μl cDNA, and 12.5 μl Taq Master mix (Beyotime Institute of Biotechnology, Haimen, China) and 8.5 μl nuclease-free water. The reaction conditions were as follows: 30 sec at 95°C

Table I. Primer sequences and product length.

Gene	Forward primer (5'-3')	Reverse primer (5'-3')	Product length (bp)
Caspase-3	TGGGTGCTATTGTGAGGCGG	GCACACCCACCGAAAACCAG	168
Cytochrome c	CGTTGTGCCAGCGACTAAAAA	GATTTGGCCCAGTCTTGTGC	129
Bcl-2	TGAACTGGGGGAGGATTGTG	AAATCAAACAGAGGCCGCAT	211
Bax	CCCAGAGGCGGGGTTTCA	GGAAAAAGACCTCTCGGGGG	207
PARP-1	GAAGCCACAGCTAGGCATGA	CGCCACTTCATCCACTCCAT	220
β-actin	GGCACCCAGCACAATGAAGA	CATCTGCTGGAAGGTGGACA	106

Bcl-2, B-cell lymphoma 2; Bax, Bcl-2 associated X protein; PARP-1, poly (adenosine 5'-diphosphate-ribose) polymerase 1.

for denaturation (1 cycle), annealing at 58°C for 30 sec and extension at 72°C for 30 sec, for a total of 35 cycles. The PCR products (10 μl) were visualized using electrophoresis on 2.0% agarose gel. The expression levels of the target mRNAs were normalized to the reference gene β-actin (22).

Western blot analysis. The cells were collected and lysed with lysis buffer (150 mM NaCl, 1.0 mM EDTA, 1% NP-40, 50 Mm Tris-HCl, pH 7.4, 1 mM phenylmethylsulfonyl fluoride, 1 μg/ml Leupeptin, 1 μg/ml aprotinin and 1 g/ml pepstatin) by incubating for 30 min at 4°C. The lysates were centrifuged at 13,500 x g for 15 min at 4°C, and the protein concentrations were determined using the Bio-Rad Protein Assay kit (Bio-Rad Laboratories, Inc.). Equal amounts of total proteins (50 μg) were mixed with loading buffer, at 95°C for 5 min, and separated on 12% SDS-PAGE gels, and then blotted onto polyvinylidene fluoride membranes. The membranes were blocked with 5% non-fat milk at room temperature for 1 h, and incubated with specific primary antibodies at room temperature for 2 h. The primary antibodies used in this study were as follows: PARP-1 antibody (1:400; sc-8007), cytochrome c antibody (1:400; sc-514435), Bcl-2 antibody (1:400; sc-509), Bax antibody (1:400; sc-4239), caspase-3 antibody (1:400; sc-136219; all from Santa Cruz Biotechnology, Inc.). All of these antibodies were rabbit monoclonal antibodies. After washing with TBST (TBS containing 0.05% Tween-20, pH 7.6) three times, the membranes were incubated with goat anti-rabbit immunoglobulin G conjugated to horseradish peroxidase (1:1,000; cat. no. Ba1055; Boster Biological Technology, Pleasanton, CA, USA) for 1 h at room temperature. Following washing with TBST three times, the proteins signal was detected using an electrochemiluminescence kit (Beyotime Institute of Biotechnology). Densitometric analyses of resultant western blots were performed with ImageJ software (ImageJ version 1.47 public domain software; National Institutes of Health, Bethesda, MD, USA).

Anti-tumor activities in vivo. Five-week old ICR male mice (weight, 18-22 g) were obtained from the Experimental Animal Center of Sichuan University (Chengdu, China). The mice were housed in an air-conditioned room, which was maintained at 23±2°C, and the relatively humidity of the house was kept at 55±5% CO_2 with a 12:12 h light/dark cycle, with free access to food and water. The CT26 cells were homogenized with NS at a ratio of (cell solution, NS=1:4; cell concentration, ~1x10⁶/ml).

The mice were injected with the cell suspension (0.2 ml/mouse) subcutaneously at the right front axilla. Once transplanted, the tumor (~50 mg) was palpable. The mice were randomly divided into different treatment groups, with 10 mice in each group. The mice in the three OSR groups were administered daily with OSR at 300, 150 and 75 mg/kg of body weight via intra-peritoneal injection (i.p). The mice in the positive control group were injected with (30 mg/kg) 5-Fu once a day, and the mice in the negative control group were administered daily with an equal volume of NS. From the third day, tumor volume (V) was measured using calipers on alternate days and calculated using the standard formula: V (mm³) = $AB^2/2$, where A is the longest superficial diameter, and B is the smallest superficial diameter. After 13 days, all mice were sacrificed by disloca-tion of cervical vertebra, and the tumor tissues were removed and weighed. Then, the tumor tissues were used to detect the expression levels of caspase-3, Bax, Bcl-2, cytochrome c and PARP-1 by RT-PCR and western blotting. The animal experi-ments were approved by the Animal Ethics Committee of the Luohe Medical College (Luohe, China).

Statistical analysis. The data are presented as the mean ± stan-dard deviation. Data were analyzed by one-way analysis of variance followed by Duncan's post-hoc test using the SPSS software package version 17.0 (SPSS, Inc., Chicago, IL, USA). $P<0.05$ was considered to indicate a statistically significant difference.

Results

OSR inhibits the proliferation of human colorectal HCT116 cancer cells. To detect the growth inhibition effects of OSR in HCT116 cells, cell growth inhibition rate, growth curve and colony-forming assays were performed. The HCT116 cells were treated with serial concentrations of OSR (3, 6, 12, 24, 48, 96 and 192 mg/l) for 48 h. The results demonstrate that the cell growth inhibition rate significantly increased in a dose-dependent manner (Fig. 2A), and that the IC_{50} value was 59.28 mg/l. The cell growth curve assay indicated that OSR may inhibit HCT116 cell growth in a time and dose-dependent manner (Fig. 2B). Compared with the negative group, the colony formation assay demonstrated that OSR may inhibit the proliferation of HCT116 cells markedly. The colony formation inhibition rate significantly increased from 51.1% for 25 mg/l OSR to 93.9% for 100 mg/l OSR (P<0.01; Fig. 3).
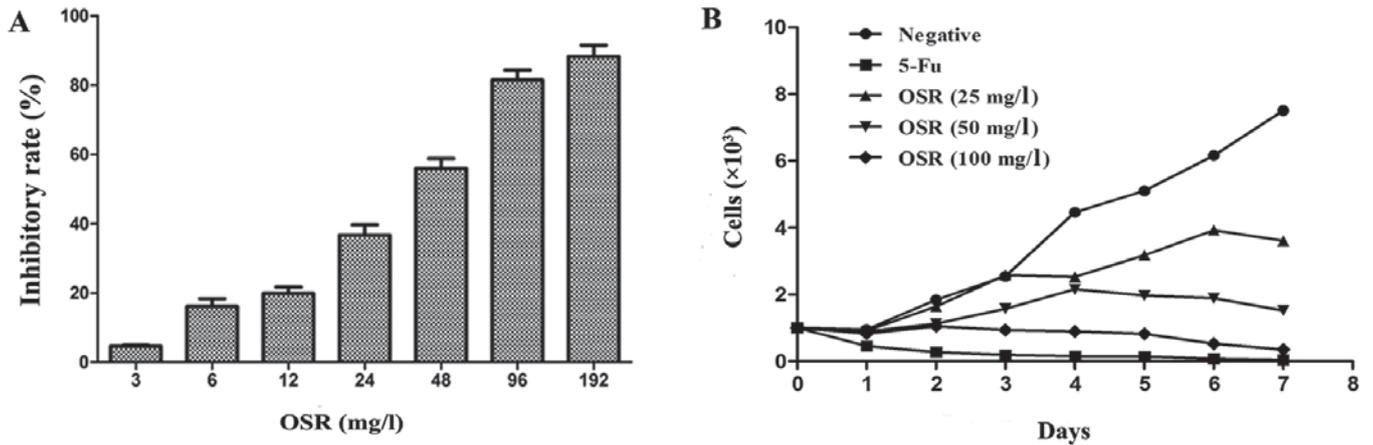
Figure 2. Effects of OSR on HCT116 cell viability. (A) HCT116 cells were treated with various concentrations (3-192 mg/l) of OSR for 48 h and then analyzed by MTT assay. (B) Growth curve of the OSR treated-HCT116 cells. The numbers of viable cells were detected by Trypan Blue staining assay after 1, 2, 3, 4, 5, 6 and 7 days of treatment. OSR, oxysophoridine.

OSR promotes apoptosis of HCT116 cells. The changes in the levels of apoptosis in OSR-treated HCT116 cells were detected via Hoechst 33258 nucleus staining. Compared with the negative group, the cells exhibited a marked increase in apoptosis following treatment with OSR for 48 h, exhibiting nuclear condensation, DNA fragmentation and the formation of apoptotic bodies. The cell apoptosis rate of the negative control group was 5.21%. Treatment with 25, 50 and 100 mg/l OSR significantly upregulated the rate of apoptosis from 46.37% (25 mg/l) to 87.62% (100 mg/l; P<0.01; Fig. 4).

OSR inhibits CRC growth in vivo. To determine whether OSR is able to inhibit tumor growth *in vivo*, CT26-xenografts were established in ICR mice. It was identified that the tumor volume of the negative control group was higher compared with the tumor volume of the OSR-treated (150 and 300 mg/kg) mice from day 9 to 13. The growth curve assay indicated that OSR was able to inhibit tumor tissue growth significantly (P<0.05, P<0.01; Fig. 5).

Effects of OSR treatmenton caspase-3, Bax, Bcl-2, cytochrome c and PARP-1expression in HCT116 cells. The levels of caspase-3, Bax, Bcl-2, cytochrome *c* and PARP-1expression in HCT116 cells were analyzed by RT-qPCR and western blotting. The HCT116 cells were treated with different concentrations of OSR (25, 50 and 100 mg/l). Compared with the control group, treatment with 50 and 100 mg/l OSR downregulated the expression of Bcl-2 and PARP-1, whereas the levels of caspase-3, Bax and cytochrome *c* were upregulated (Fig. 6).

Effects of OSR treatment on caspase-3, Bax, Bcl-2, cytochrome c and PARP-1expression in transplanted CT26CRC tissues. The caspase-3, Bax, Bcl-2, cytochrome *c* and PARP-1 expression levels in the transplanted CT26CRC tissues were also detected by RT-PCR and western blot analysis. Compared with the negative control group, the levels of Bcl-2 and PAPR-1 were significantly decreased in cells treated with 150 and 300 mg/kg OSR, and the levels of caspase-3, Bax and cytochrome *c* were increased in the OSR groups (150 and 300 mg/kg; Fig. 7).
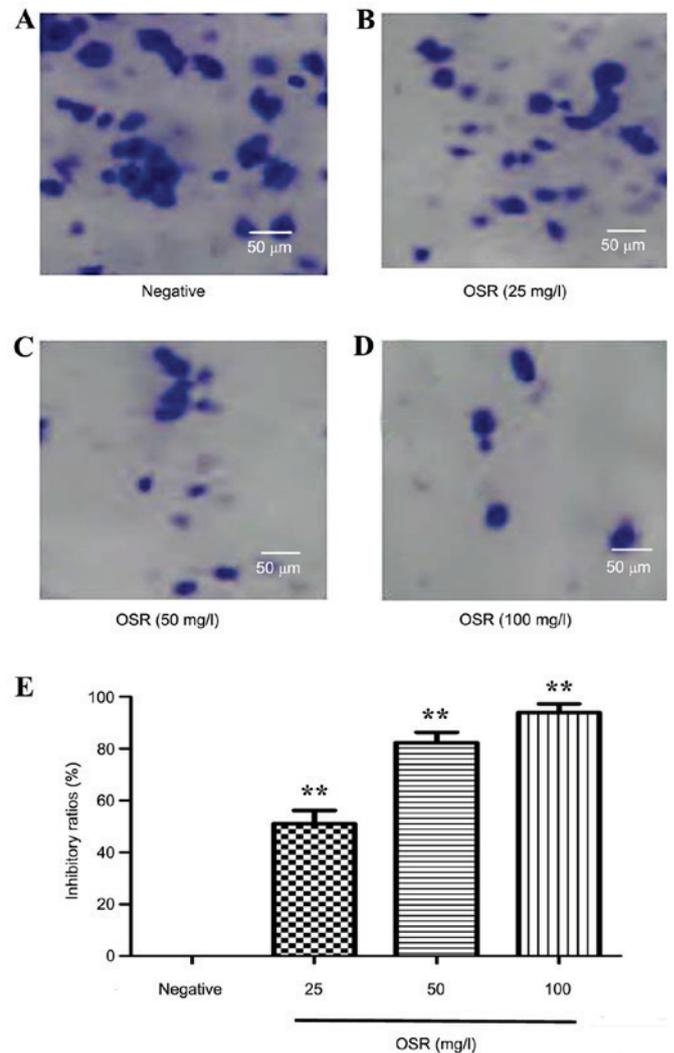
Figure 3. OSR inhibits colony formation of HCT116 cells. (A) Negative control group; (B) OSR 25 mg/l; (C) OSR 50 mg/l and (D) OSR 100 mg/l. (E) Graph indicating the colony formation inhibitory rate. HCT116 cells were treated with various concentrations of OSR (25, 50 and 100 mg/l) for 14 days. The number of colonies formed was subsequently counted, and the colony formation inhibitory rate was calculated. The inhibitory rate increased from 51.1% where the cells were treated with 25 mg/l OSR to 93.9% where 100 mg/l OSR was used. **P<0.01 vs. the negative group. OSR, oxysophoridine.
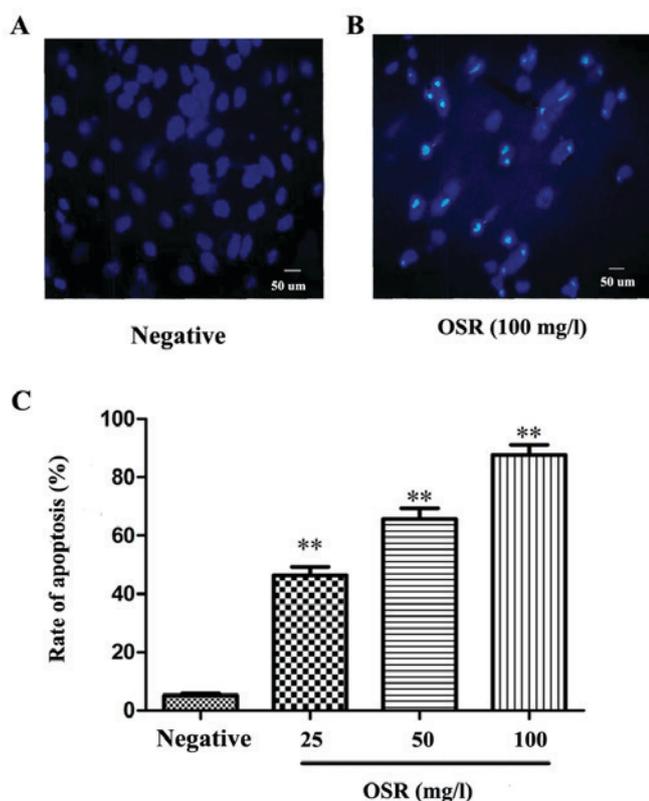
Figure 4. Apoptosis was detected by Hoechst 33258 staining (magnification, x200). (A) Negative control group; (B) OSR 100 mg/l; (C) the HCT116 cells exhibited significantly increased levels of apoptosis following treatment with OSR (25, 50 and 100 mg/l) for 48 h vs. negative group. **P<0.01 vs. the negative group. OSR, oxysophoridine.

Figure 5. OSR inhibited the colorectal tumor growth *in vivo*. (A) Growth curve (the tumor volume) showed that OSR could inhibit the mouse CT26 transplantable colorectal tumor tissue volume significant; (B) OSR inhibited the tumor weight (the 13th day). *P<0.05, **P<0.01 vs. the control group. OSR, oxysophoridine; 5-Fu, fluorouracil.

Discussion

Colorectal cancer is one of the most common digestive tract malignancies worldwide, with a poor prognosis (23). Apoptosis or programmed cell death (PCD) is a mechanism of nucleated cell death, which is regulated by physiological processes, including alterations to the intracellular and extracellular environments or cell death signaling activation. Cell membrane shrinkage, nucleus pyknosisorkaryolysis, DNA fragmentation and formation of apoptotic bodies are characteristics of apoptotic cells. A number of previous studies indicated that cellular apoptosis was associated with the occurrence, development, therapy and prognosis of numerous types of human tumor (24-26). To the best of our knowledge, apoptin plays a paramount role in apoptosis, by upregulating pro-apoptotic proteins (caspase-3, cytochrome *c*, and Bax) and downregulating anti-apoptotic proteins (Bcl-2 and PARP-1) (27-34). Previous studies have indicated that increased Bax expression may induce apoptosis and that increased Bcl-2 expression may inhibit apoptosis (35). Caspase-3, belongs to the family of cysteine proteases, and is a crucial mediator of apoptosis. Caspases are divided into three broad categories: Apoptotic initiators (caspase-2, -8, -9 and -10), apoptotic inhibitors (caspase-3, -6 and -7) and inflammatory mediators (caspase-1, -4, -5 and -11) (36,37). To date, multiple previous studies have demonstrated that caspase-3 is a major effector in the process of apoptosis, and that its activation marks the irreversible stage of apoptosis (38). The release of cytochrome *c* in the

mitochondria is one of the inchoate diagnostic characteristics in nucleated cell apoptosis (39). Bcl-2 inhibits cell apoptosis by reducing the release of mitochondrial cytochrome *c* in order to inhibit the activation of caspase-3. Bax protein, as a crucial component of mitochondrial membrane ion channels, induces the transfer of cytochrome *c* across mitochondrial membranes and the formation of apoptotic bodies; activates caspase-9 andcaspase-3, which consequently leads to apoptosis (40). PARP-1 is a type of post-translational modification protein enzyme, which exists in the cell nucleus and cytoplasm and is involved in DNA damage repair, gene transcription regulation, telomerase activity regulation and protein degradation. PAPR-1 is cleaved into two fragments, p89 and p24, by caspase-3, which causes a loss of PARP-1 function and leads to apoptosis (41-44).

In the present study, the inhibitory effects of OSR on the proliferation of the human CRC HCT116 cells were detected. Cell growth inhibition, growth curve and colony-forming assays indicated that treatment with OSR was able to inhibit the growth of HCT116 cells in a time and dose-dependent manner. Hoechst 33258 staining demonstrated that OSR was able to induce apoptosis inHCT116 cells. An antitumor effect of OSR on CRC in a mouse model of transplanted CT26 CRC was also observed. Furthermore, it was observed that OSR was able to significantly inhibit the growth of tumors at doses of 150 and 300 mg/kg/day. Concomitantly, in order to additionally investigate the mechanism of OSR-induced apoptosis, the expression levels of apoptotic-associated proteins were detected *in vivo* and *in vitro*. The results demonstrated that treatment with
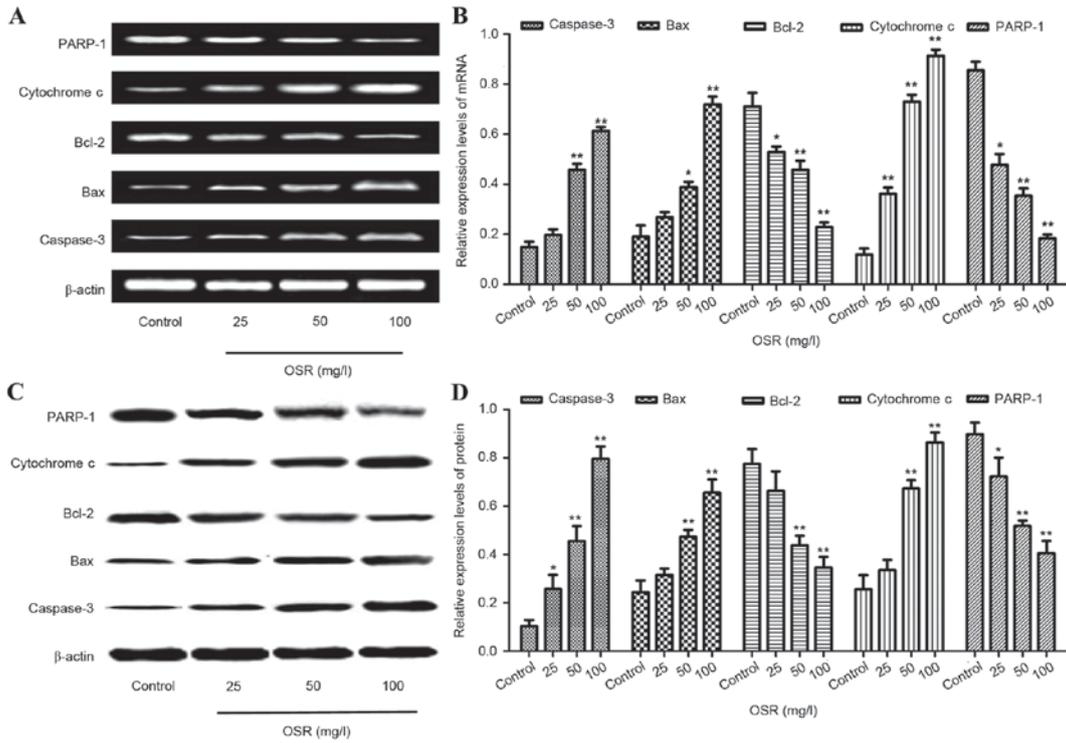
Figure 6. OSR upregulates the levels of caspase-3, Bax and cytochrome *c* expression, and downregulates the levels of Bcl-2 and PARP-1 in the HCT116 cells. (A and B) The levels of caspase-3, Bax, cytochrome *c*, Bcl-2 and PARP-1 mRNA expression in HCT116 cells. (C and D) The levels of caspase-3, Bax, cytochrome *c*, Bcl-2 and PARP-1 protein in HCT116 cells. $^*P<0.05$, $^{**}P<0.01$ vs. the control group. OSR, oxysophoridine; Bcl-2, B-cell lymphoma 2; Bax, Bcl-2 associated X protein; PARP-1, poly (adenosine 5'-diphosphate-ribose) polymerase 1.
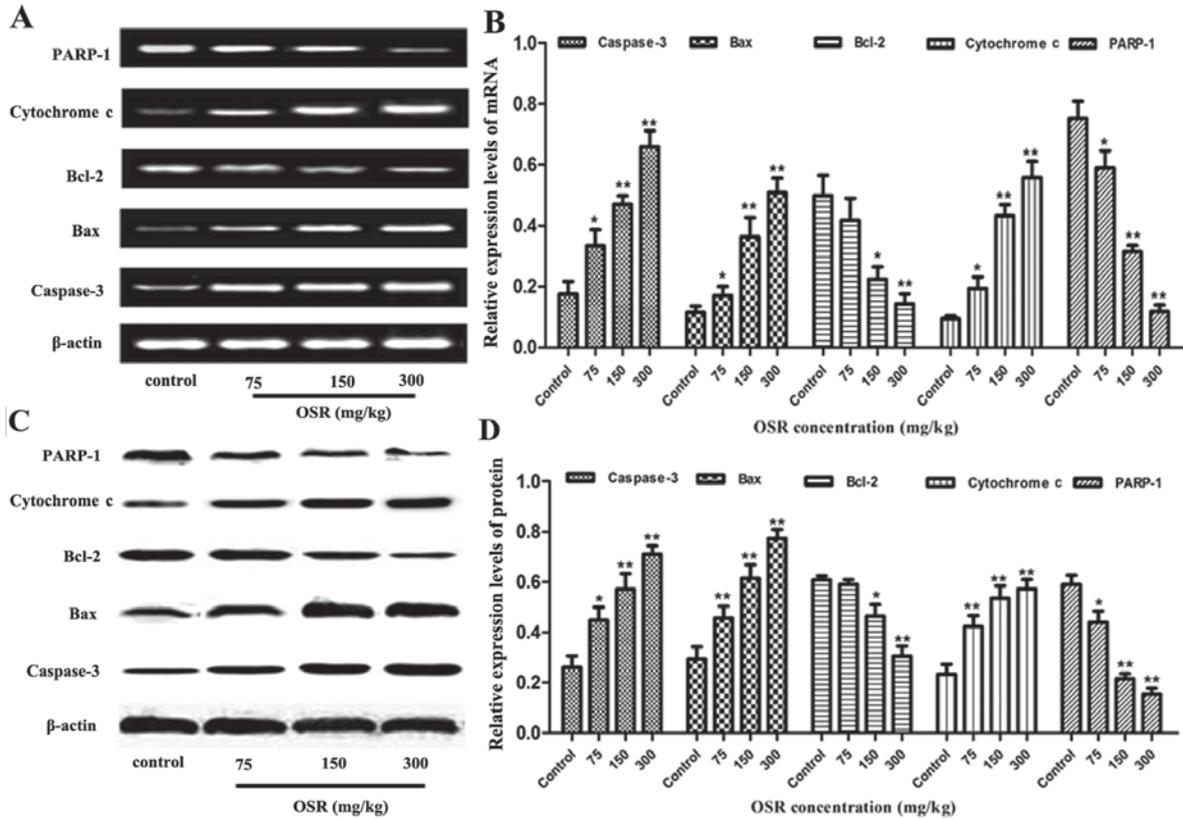
Figure 7. OSR upregulates the levels of caspase-3, Bax and cytochrome *c* expression, and downregulates the levels of Bcl-2 and PARP-1 expression in the transplanted mouse CT26 colorectal cancer tissues. (A and B) The levels of caspase-3, Bax, cytochrome *c*, Bcl-2 and PARP-1 mRNA expression in the transplanted mouse CT26 colorectal cancer tissues. (C and D) The levels of caspase-3, Bax, cytochrome *c*, Bcl-2 and PARP-1 protein in transplanted mouse CT26 colorectal cancer tissues. $^*P<0.05$, $^{**}P<0.01$ vs. the control group. OSR, oxysophoridine; Bcl-2, B-cell lymphoma 2; Bax, Bcl-2 associated X protein; PARP-1, poly (adenosine 5'-diphosphate-ribose) polymerase 1.

OSR was able to suppress Bcl-2 and PARP-1 expression, and augment caspase-3, Bax and cytochrome *c* expression.

Therefore, the present study concluded that OSR is able to mediate anti-tumor activity in CRC cells *in vivo* and *in vitro*, via the induction of apoptosis, and its mechanism may be associated with the Bcl-2/Bax/caspase-3 signaling pathway.

Acknowledgements

References

1. Ferlay J, Soerjomataram I, Dikshit R, Eser S, Mathers C, Rebelo M, Parkin DM, Forman D and Bray F: Cancer incidence and mortality worldwide: Sources, methods and major patterns in GLOBOCAN 2012. Int J Cancer 136: E359-E386, 2015.
2. Young GP, Senore C, Mandel JS, Allison JE, Atkin WS, Benamouzig R, Bossuyt PM, Silva MD, Guittet L, Halloran SP, *et al*: Recommendations for a step-wise comparative approach to the evaluation of new screening tests for colorectal cancer. Cancer 122: 826-839, 2016.
3. Aykan NF: Red meat and colorectal cancer. Oncol Rev 9: 288, 2015.
4. Martinez-Useros J and Garcia-Foncillas J: Obesity and colorectal cancer: Molecular features of adipose tissue. J Transl Med 14: 21, 2016.
5. Cetinkaya E, Dogrul AB and Tirnaksiz MB: Role of self-expandable stents in management of colorectal cancers. World J Gastrointest Oncol 8: 113-120, 2016.
6. Palma S, Zwenger AO, Croce MV, Abba MC and Lacunza E: From molecular biology to clinical trials: Toward personalized colorectal cancer therapy. Clin Colorectal Cancer 15: 104-115, 2016.
7. Buckley H, Wilson C and Ajithkumar T: High-dose-rate brachytherapy in the management of operable rectal cancer: A systematic review. Int J Radiat Oncol Biol Phys 99: 111-127, 2017.
8. Hammond WA, Swaika A and Mody K: Pharmacologic resistance in colorectal cancer: A review. Ther Adv Med Oncol 8: 57-84, 2016.
9. Chibaudel B, Tournigand C, Bonnetain F, Richa H, Benetkiewicz M, André T and de Gramont A: Therapeutic strategy in unresectable metastatic colorectal cancer: An updated review. Ther Adv Med Oncol 7: 153-169, 2015.
10. Lu X, Li Y, Li X and Aisa HA: Luteolin induces apoptosis in vitro through suppressing the MAPK and PI3K signaling pathways in gastric cancer. Oncol Lett 14: 1993-2000, 2017.
11. Li B, Chen D, Li W and Xiao D: 20(S)-Protopanaxadiol saponins inhibit SKOV3 cell migration. Oncol Lett 11: 1693-1698, 2016.
12. Chang A, Cai Z, Wang Z and Sun S: Extraction and isolation of alkaloids of Sophora alopecuroides and their anti-tumor effects in H22 tumor-bearing mice. Afr J Tradit Complement Altern Med 11: 245-248, 2014.
13. Wang CZ, Zhang Z, Anderson S and Yuan CS: Natural products and chemotherapeutic agents on cancer: Prevention vs. treatment. Am J Chin Med 42: 1555-1558, 2014.
14. Park GH, Park JH, Song HM, Eo HJ, Kim MK, Lee JW, Lee MH, Cho KH, Lee JR, Cho HJ and Jeong JB: Anti-cancer activity of Ginger (*Zingiber officinale*) leaf through the expression of activating transcription factor 3 in human colorectal cancer cells. BMC Complement Altern Med 14: 408, 2014.
15. Meng C, Liu C, Liu Y and Wu F: Oxysophoridine attenuates the injury caused by acute myocardial infarction in rats through anti-oxidative, anti-inflammatory and anti-apoptotic pathways. Mol Med Rep 11: 527-532, 2015.
16. Wang YS, Li YX, Zhao P, Wang HB, Zhou R, Hao YJ, Wang J, Wang SJ, Du J, Ma L, *et al*: Anti-inflammation effects of oxysophoridine on cerebral ischemia-reperfusion injury in mice. Inflammation 38: 2259-2268, 2015.
17. Yang G, Gao J, Jia Y, Yan L, Yu J and Jiang Y: Oxysophoridine through intrathecal injection induces antinociception and increases the expression of the GABAAa1 receptor in the spinal cord of mice. Planta Med 78: 874-880, 2012.
18. Yao XQ, Zhang YH, Long W and Liu PX: Oxysophoridine suppresses the growth of hepatocellular carcinoma in mice: In vivo and cDNA microarray studies. Chin J Integr Med 18: 209-213, 2012.
19. Yu J, Li Y, Zhao C, Gong X, Liu J, Wang F and Jiang Y: Effect of oxysophoridine on electric activities and its power spectrum of reticular formation in rats. Zhongguo Zhong Yao Za Zhi 35: 1170-1172, 2010 (In Chinese).
20. Zhang HM and Li HQ: Anti-arrhythmic effects of sophoridine and oxysophoridine. Zhongguo Yao Li Xue Bao 20: 517-520, 1999.
21. Zhang JT, Zhou WL, He C, Liu T, Li CY and Wang L: 5-Fluorouracil induces apoptosis of colorectal cancer cells. Genet Mol Res 15: 15017326, 2016.
22. Little EC, Kubic JD, Salgia R, Grippo PJ and Lang D: Canonical and alternative transcript expression of PAX6 and CXCR4 in pancreatic cancer. Oncol Lett 13: 4027-4034, 2017.
23. Aakif M, Balfe P, Elfaedy O, Awan FN, Pretorius F, Silvio L, Castinera C and Mustafa H: Study on colorectal cancer presentation, treatment and follow-up. Int J Colorectal Dis 31: 1361-1363, 2016.
24. Bold RJ, Termuhlen PM and McConkey DJ: Apoptosis, cancer and cancer therapy. Surg Oncol 6: 133-142, 1997.
25. Scatena R: Mitochondria and cancer: A growing role in apoptosis, cancer cell metabolism and dedifferentiation. Adv Exp Med Biol 942: 287-308, 2012.
26. Elkholi R, Renault TT, Serasinghe MN and Chipuk JE: Putting the pieces together: How is the mitochondrial pathway of apoptosis regulated in cancer and chemotherapy? Cancer Metab 2: 16, 2014.
27. Yang D, Okamura H, Teramachi J and Haneji T: Histone demethylase Jmjd3 regulates osteoblast apoptosis through targeting anti-apoptotic protein Bcl-2 and pro-apoptotic protein Bim. Biochim Biophys Acta 1863: 650-659, 2016.
28. Luna-Vargas MP and Chipuk JE: The deadly landscape of pro-apoptotic BCL-2 proteins in the outer mitochondrial membrane. FEBS J 283: 2676-2689, 2016.
29. Um HD: Bcl-2 family proteins as regulators of cancer cell invasion and metastasis: A review focusing on mitochondrial respiration and reactive oxygen species. Oncotarget 7: 5193-5203, 2016.
30. Lalier L, Cartron PF, Juin P, Nedelkina S, Manon S, Bechinger B and Vallette FM: Bax activation and mitochondrial insertion during apoptosis. Apoptosis 12: 887-896, 2007.
31. HorwacikI and Rokita H: Targeting of tumor-associated gangliosides with antibodies affects signaling pathways and leads to cell death including apoptosis. Apoptosis 20: 679-688, 2015.
32. Ishii Y, Nhiayi MK, Tse E, Cheng J, Massimino M, Durden DL, Vigneri P and Wang JY: Knockout serum replacement promotes cell survival by preventing BIM from inducing mitochondrial cytochrome C release. PLoS One 10: e0140585, 2015.
33. Węsierska-Gądek J, Mauritz M, Mitulovic G and Cupo M: Differential potential of pharmacological PARP inhibitors for inhibiting cell proliferation and inducing apoptosis in human breast cancer cells. J Cell Biochem 116: 2824-2839, 2015.
34. Dias MM, Noratto G, Martino HS, *et al*: Pro-apoptotic activities of polyphenolics from açaí (*Euterpe oleracea* Martius) in human SW-480 colon cancer cells. Nutr Cancer 66: 1394-1405, 2014.
35. Zheng JH, Viacava Follis A, Kriwacki RW and Moldoveanu T: Discoveries and controversies in BCL-2 protein-mediated apoptosis. FEBS J 283: 2690-2700, 2016.
36. Julien O and Wells JA: Caspases and their substrates. Cell Death Differ 24: 1380-1389, 2017.
37. Yuan J, Najafov A and Py BF: Roles of caspases in necrotic cell death. Cell 167: 1693-1704, 2016.
38. Fiandalo MV and Kyprianou N: Caspase control: Protagonists of cancer cell apoptosis. Exp Oncol 34: 165-175, 2012.
39. Caroppi P, Sinibaldi F, Fiorucci L and Santucci R: Apoptosis and human diseases: Mitochondrion damage and lethal role of released cytochrome C as proapoptotic protein. Curr Med Chem 16: 4058-4065, 2009.
40. Zhao Y, Jing Z, Lv J, Zhang Z, Lin J, Cao X, Zhao Z, Liu P and Mao W: Berberine activates caspase-9/cytochrome c-mediated apoptosis to suppress triple-negative breast cancer cells in vitro and in vivo. Biomed Pharmacother 95: 18-24, 2017.
41. Koh DW, Dawson TM and Dawson VL: Mediation of cell death by poly(ADP-ribose) polymerase-1. Pharmacol Res 52: 5-14, 2005.
42. Yu SW, Wang H, Poitras MF, Coombs C, Bowers WJ, Federoff HJ, Poirier GG, Dawson TM and Dawson VL: Mediation of poly(ADP-ribose) polymerase-1-dependent cell death by apoptosis-inducing factor. Science 297: 259-263, 2002.
43. Schon EA and Manfredi G: Neuronal degeneration and mitochondrial dysfunction. J Clin Invest 111: 303-312, 2003.
44. Voutsadakis IA: Apoptosis and the pathogenesis of lymphoma. Acta Oncol 39: 151-156, 2000.